

## Optimization on configuration of surface conduction electron-emitters

Hui-Wen Cheng<sup>a</sup>, Yiming Li<sup>a,b,\*</sup>

<sup>a</sup> Department of Electrical Engineering and Institute of Communications Engineering, National Chiao Tung University, 1001 Ta-Hsueh Road, Hsinchu 300, Taiwan

<sup>b</sup> National Nano Device Laboratories, Hsinchu 300, Taiwan

### ARTICLE INFO

#### Article history:

Received 29 November 2009

Received in revised form 8 January 2010

Available online 23 March 2010

### ABSTRACT

In this work, a novel nanogap with inclined protrusion cathode in palladium strip fabricated by hydrogen absorption under high-pressure treatment is optimized for the surface conduction electron-emitter. Its field emission is sensitive to the geometry of surface conduction electron-emitters (SCE). For a specified emitter material, the SCE are further investigated by varying the thickness, tilted angle and gap of palladium (Pd). An optimal field emission efficiency with 80° tilted angle, 120 nm gap and 10 nm thickness of Pd is found for certain designed field emission efficiency. We further find that varying the emitter material work function of the emitter material from 5.12 eV to 3.9 eV will further improve the field emission property due to the increase of the emitted current.

© 2010 Elsevier Ltd. All rights reserved.

### 1. Introduction

Electrodes with nanometer separation have lots of different applications, such as molecular electronics [1,2] and vacuum microelectronics [3]. One of emerging technologies of nanogap is the surface conduction electron-emitter (SCE) [4] for the flat panel displays (FPDs) applications which has attracted much attention since reported by Sakai et al. [5]. The SCE display (SED) is an advanced type of FPD based upon SCEs. The critical process step to fabricate SCEs is to create a nanofissure on a line electrode for the electron emission. SEDs have some attractive advantages, such as high-quality image, high resolution, quick response time, as well as low power consumption [6]. However, the nanogap fabrication process is such complicated and expensive. We notice that the field emission (FE) efficiency and current density of these FE cathodes further depend on both their geometry and fabrication materials. For the SCE, emission is obtained with a large electric field by a driving voltage that causes electrons to tunnel over a potential barrier out of the emitter to the driving electrode and anode. The emitter's geometry increases emission by enhancing the electric field and reducing the barrier over which the electrons must tunnel.

In this work, we theoretically optimized the fabricated a palladium (Pd) nanogap electrode with a well-defined gap size [7,8]. For a fixed emitter material work function, the SCEs are investigated by varying the thickness, the tilted angle and the gap of palladium (Pd). Optimal field emission efficiency with 80° tilted angle,

120 nm gap and 10 nm thickness of Pd could be found. We have found that the proposed SCE with a smaller emitter material work function for the emitter material will induce a larger emitted current, which may increase the collected current on the anode. It possesses higher field emission with higher focusing capability, compared with proposed SCE with a larger work function of Pd in the part of cathode, as shown in Fig. 1.

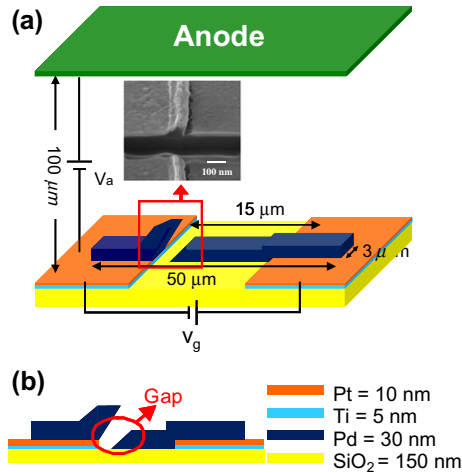
### 2. Structure and simulation

Fig. 1a schematically shows the structure of FPD based upon SCEs. Firstly, the substrate is formed by a p-type (100) silicon (Si) wafer. On silicon substrate, a 150-nm-thick SiO<sub>2</sub> layer was thermally grown. An adhesion layer which was made by titanium (Ti) with 5-nm-thick is deposited by electron-beam-evaporation (e-beam) on the oxide. On the top of titanium, the Platinum (Pt) with a 10 nm thickness thin film is as well as deposited by e-beam. By a lift-off process, the pattern of Pt/Ti line electrodes with 80 μm width was photolithographically performed. On the Pt/Ti bottom electrode, the Pd with 30 nm thickness thin film [9,10] was deposited by e-beam. And the lift-off method was also used to pattern the Pd electrode line of 50 μm length and 3-μm width [11–13]. Under high-pressure treatment, a nanogap with a separation on the Pd strip was then produced by hydrogen absorption. About the anode, we use screen printing to obtain phosphor thick films. Then the aluminium coating with the thickness of 50–300 nm was evaporated on some phosphor films. A clear description of fabrication and characterization could be found in our previous work [14,15].

For investigating the field emission properties in SCE, the FDTD-PIC [16–19] codes are implemented. Starting from a specified initial state, we simulate electrostatic fields as its evolution in time.

\* Corresponding author. Address: Department of Electrical Engineering, National Chiao Tung University, 1001 Ta-Hsueh Road, Hsinchu 300, Taiwan. Tel.: +886 35712121x52974.

E-mail address: [yml@faculty.nctu.edu.tw](mailto:yml@faculty.nctu.edu.tw) (Y. Li).



**Fig. 1.** (a) Schematic plot of the SED structure and (b) the cross-sectional plot on the  $xz$  plane. The distance between anode and cathode is  $100\ \mu\text{m}$ . The gate voltage ( $V_g$ ) and anode voltage ( $V_a$ ) are  $40\ \text{V}$  and  $1200\ \text{V}$  respectively [7].

We then perform a time integration of Faraday's law, Ampere's law, and the relativistic Lorentz equation. The full set of Maxwell time-dependent equations is simultaneously solved to obtain electromagnetic fields. Similarly, the Lorentz force equation is solved to obtain the relativistic particle trajectories. In addition, the electromagnetic fields are advanced in time at each time step. The charged particles are moved according to the Lorentz equation using the fields advanced in each time step. The weighted charge and current density at the grids are subsequently calculated. The obtained charge and current densities are successively used as sources in the 3D Maxwell equations for advancing the electromagnetic fields. These steps are repeated for each time step until the final time is reached. In addition, the FDTD-PIC method allows the statistical representation of general distribution functions in phase space. The use of fundamental equations contains the full nonlinear effects, the space charge and other collective effects which can be included self-consistently by coupling charged particles to the field equations via source terms. The particle treatment permits the incorporation of relativistic effects. This 3D FDTD-PIC method approaches a self-consistent simulation of the electromagnetic fields and charged particles. In the FE process, the electron emission is modelled using the Fowler–Nordheim (F–N) equation. We notice that all dimensions of the physical quantities are the same with the experimental settings and the surfaces in the SCE are assumed to be smooth on the cell level in the complete simulation [7,8,16,18].

### 3. Results and discussion

To explore the electron-emission behaviours in SCEs, the FDTD-PIC simulation technique [16–19] is employed to solve a set of 3D

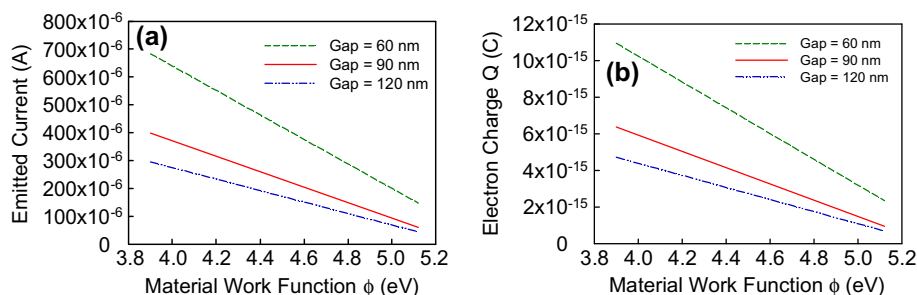


**Fig. 2.** (a) The effect of emitter material work function on the field emission current with various separation of nanogap. (b) The corresponding electron charges of the field emission in (a).

Maxwell equations coupled with the Lorentz equation. Including the effect of space charge, this approach is a self-consistent simulation of the electromagnetic fields and charged particles. In the FE process, the electron emission is modelled by F–N equation. We found that the proposed SCE with  $3.9\ \text{eV}$  emitter material work function has higher emitted emission than with  $5.12\ \text{eV}$  emitter material work function which is based on experimental data, as shown in Figs. 2, 4 and 6, respectively.

Fig. 2a shows the effect of emitter material work function on the field emission current with 60-, 90- and 120-nm separations of nanogap. The emitted current decreases as the nanogap become wider due to electric field degrading. Fig. 2b shows the corresponding electron charges of the field emission in Fig. 2a, which is proportional to the emitted current. The emitted current with 60 nm gap is larger than that of 90 nm and 120 nm due to the stronger electric field, as shown in Fig. 3a. As the separation is increased, the electrical field is weakened. The results show that SCE with larger nanogap leads narrow distribution of electric field and number of emitted electrons extracted from tip of emitter is restricted, as shown in Fig. 3b. With a smaller tilted angle, the tip of emitter benefits enhancement of electrical field and emits more electrons out, as shown in Fig. 4a, where the tilted angle is  $20^\circ$ ,  $50^\circ$  and  $80^\circ$  respectively. The corresponding electron charges of the field emission are shown in Fig. 4b. The SCE with a larger tilted angle benefits emitted electrons to move upward, but obtuse angle is detrimental for electric field to emit more electrons out from emitter, as shown in Fig. 5a and b, which results in narrow distribution of electric field. Then the collected current on the anode is decreased and the field emission efficiency becomes lower. Fig. 6a and b shows the effects of the emitter material work function on the field emission current and corresponding electron charges with the thickness of the 10, 30 and 50 nm nanogap, respectively. Fig. 7a shows the thin thickness of Pd provides a larger emitted current than a thicker one due to the tip formation around emitters. The thicker thickness of Pd is harmful to tip formation around emitter so that has lack of emitted electrons, as shown in Fig. 7b. According to above analysis, we change the thickness (10, 20 and 30 nm), tilted angle ( $20^\circ$ ,  $50^\circ$ ,  $80^\circ$ ) and gap (60, 90 and 120 nm) of Pd with smaller emitter material work function simultaneously to investigate field emission. For example, the SCE with 60 nm gap, 10 nm thickness and tilted angle  $20^\circ$  benefits the tip formation around emitter, but most emitted electrons may be attracted by the strong electrical field to move downward that results in smaller collected current on the anode. Although the reduction of collected current is large, the SCE with Fig. 7a shows the thin thickness of Pd provides a larger emitted current than a thicker one due to the tip formation around emitters. The thicker thickness of Pd is harmful to tip formation around emitter so that has lack of emitted electrons, as shown in Fig. 7b. According to above analysis, we change the thickness (10, 20 and 30 nm), tilted angle ( $20^\circ$ ,  $50^\circ$ ,  $80^\circ$ ) and gap (60, 90 and 120 nm) of Pd with smaller emitter material work function simultaneously to investigate field emission. For example, the

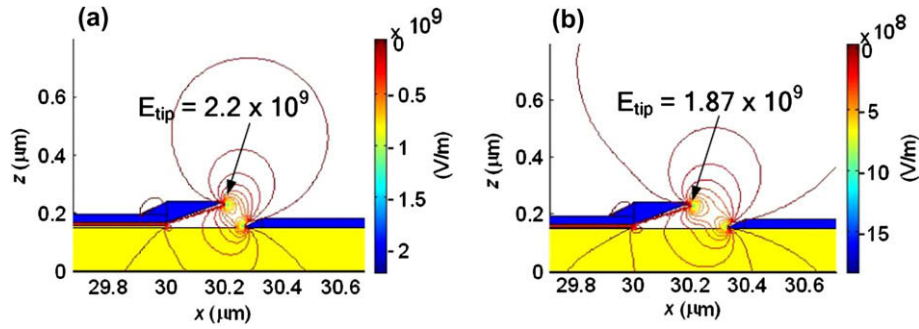


**Fig. 3.** The contour of the electric field for the structure with (a) 60 nm gap, 20° tilted angle and 10 nm thickness of Pd and with (b) 120 nm gap, 20° tilted angle and 10 nm thickness of Pd at  $V_g = 40$  V.

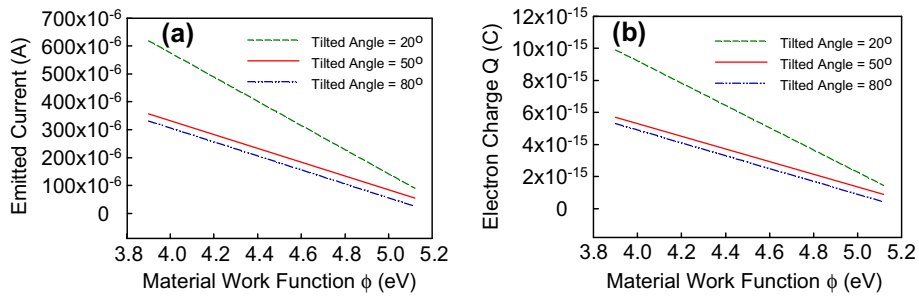


**Fig. 4.** (a) The effect of emitter material work function on the field emission current with various tilted angle of nanogap. (b) The corresponding electron charges of the field emission in (a).

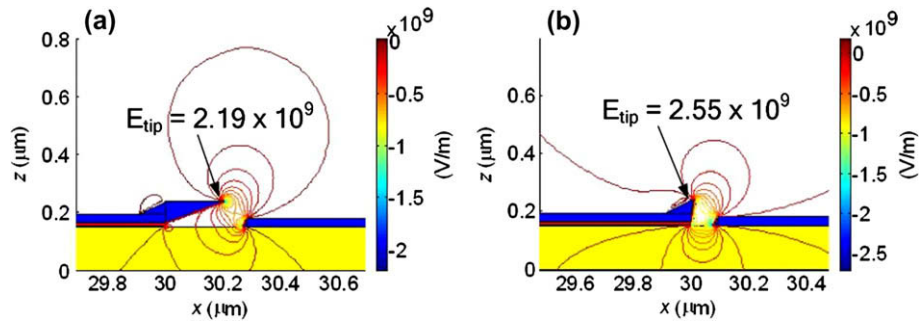


**Fig. 5.** The contour of the electric field for the structure with (a) 60 nm gap, 20° tilted angle and 30 thickness of Pd and with (b) 60 nm gap, 80° tilted angle and 30 thickness of Pd at  $V_g = 40$  V.

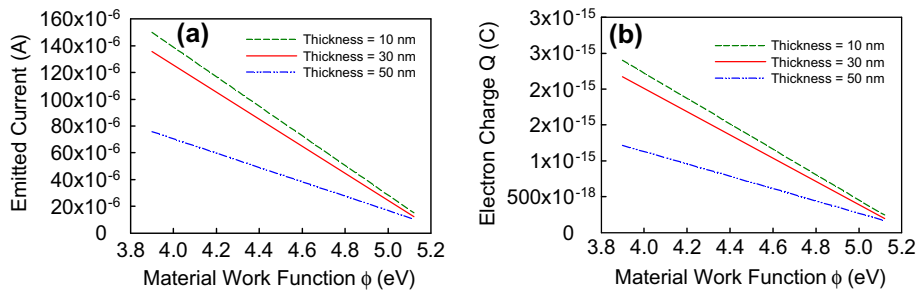


**Fig. 6.** (a) The effect of emitter material work function on the field emission current with various thickness of nanogap. (b) The corresponding electron charges of the field emission in (a).

SCE with 60 nm gap, 10 nm thickness and tilted angle 20° benefits the tip formation around emitter, but most emitted electrons may be attracted by the strong electrical field to move downward that

results in smaller collected current on the anode. Although the reduction of collected current is large, the SCE with a smaller work function cause more electrons can tunnel through material due to

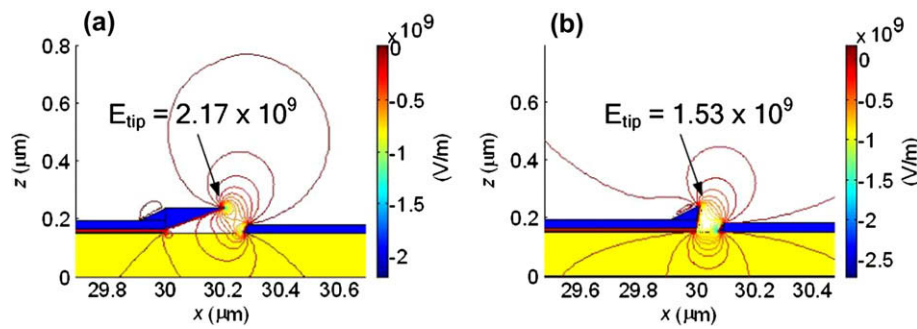


**Fig. 7.** The contour of the electric field for the structure with (a) 120 nm gap, 50° tilted angle and 10 nm thickness of Pd and with (b) 120 nm gap, 50° tilted angle and 50 nm thickness of Pd at  $V_g = 40$  V.

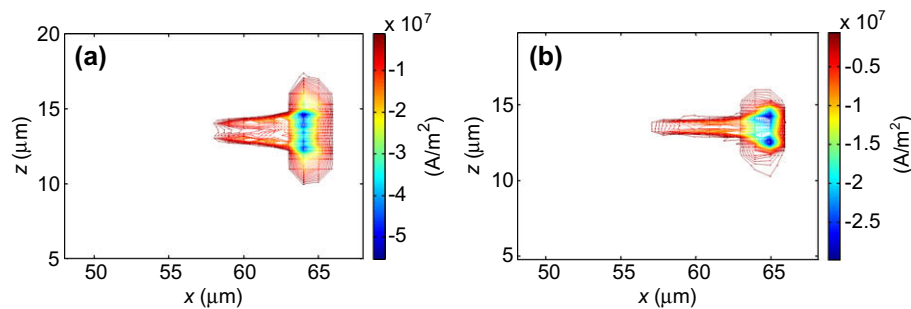


**Fig. 8.** The simulated current density distributions on the anode plates for the SCE structures (a) with 60 nm gap, 10 nm thickness and 20° tilted angle and (b) with 120 nm gap, 10 nm thickness and 50° tilted angle.

lower barrier. In analysis the field emission, it is more clear and convenient to check the field emission efficiency ( $\eta$ ) which is defined as the ratio of the collected currents on the anode ( $I_c$ ) and emitted current ( $I_e$ ). It implies that the field emission efficiency is proportional to the collected current on the anode and inversely proportional to emitted current. For the case of 60 nm gap, 10 nm thickness and 20° tilted angle, both design conditions (narrower gap, thin thickness and smaller tilted angle) benefit the enhancement of electric field. The emitted current becomes large but the strong electric field attracts more emitted electrons to move downward so that collected current on the anode is reduced, as shown in Fig. 8a. Then it results in smaller field emission efficiency but with larger emitted current. With 10 nm gap, 120 nm thickness and 50° tilted angle, the wider gap may reduce the emitted current and weaken the electric field. A larger tilted angle exhibits a smaller collected current on the anode due to smaller emitted electrons, as shown in Fig. 8b. However, weak electric field attracts less emitted electrons to move downward so that more electrons can move upward. Therefore, the field emission efficiency is increased.

#### 4. Conclusions

The electron emission properties in the novel SCE palladium nanogap fabricated by high-pressure hydrogen absorption treatment have been comprehensively explored. The new SCE has the protrusion on the cathode and the inclined sidewall, and these key features enhance the local fields and electron beam focuses; they thus protect emission areas from being damaged by impurity ions during FE operation. The result has shown that SCE with smaller emitter material work function has high FE efficiency, low turn-on voltages and high focusing capability, compared with SCE using larger work function. Through the time-dependent FDTD-PIC simulation, a beneficial design for setting of SCE geometry is with

50–80° tilted angle, 90–120 nm gap and 10–30 nm thickness of Pd. Consequently, optimal and reliable field emission efficiency with 80° tilted angle, 120 nm gap and 10 nm thickness of Pd has been found. The results of this study allow us to precisely control the current density distributions on the anode plates for designing high-quality SCE display.

We note that the Pd–H system has two distinct phases, a hydrogen solution phase  $\alpha$  and a hydride phase  $\beta$ . The two phases may singly exist in a pure form or coexist in the Pd–H system depending on the Pd:H atomic ratio and the absorption temperature. The  $\beta$  phase has a lattice constant larger than the  $\alpha$  phase. The phase transformation from  $\alpha$  phase to  $\beta$  phase is accompanied by a volume expansion of 12%, resulting in a large compressive stress in the Pd thin film. Under this consideration, we use high-pressure hydrogen treatment to form one single nanogap in the Pd strip electrode of the explored SCE structure. Based upon our theoretical results, shown in Figs. 2, 4 and 6, an experimental work is currently under planned which will be conducted in our future work.

#### Acknowledgement

This work was supported in part by Taiwan National Science Council (NSC) under NSC-97-2221-E-009-154-MY2 and Contract NSC-96-2221-E-009-210.

#### References

- [1] Reed MA, Zhou C, Muller CJ, Burgin TP, Tour JM. Conductance of a molecular junction. *Science* 1997;278:252–5.
- [2] Linag W, Shores MP, Bockrath M, Long JR, Park H. Kondo resonance in a single-molecule transistor. *Nature* 2002;417:725–9.
- [3] Lee HI, Park SS, Park DI, Ham SH, Lee JH. Nanometer-scaled gap control for low voltage and high current operation of field emission array. *J Vac Sci Technol B* 1998;16:762–4.
- [4] Nomura, Sakai K, Yamaguchi E, Yamanobe M, Ikeda S, Hara T, et al. A new emissive display based on surface-conduction electron-emitters. In: *Proc of IDW*; 1996. p. 523–6.

- [5] Sakai K, Nomura I, Yamaguchi E, Yamanobe M, Ikeda S, Hara T, et al. Fabrication and characterization of a nanogap edge emitter with a silicon-on-insulator wafer. In: Proc of EuroDisplay '96, vol. 18; 1996. p. 569–72.
- [6] Yamaguchi E, Sakai K, Nomura I, Ono T, Yamanobe M, Abe N, et al. A 10-in. surface-conduction electron-emitter display. *J Soc Inform Display* 1997;5: 345–8.
- [7] Lo HY, Li Y, Chao HY, Tsai CH, Pan FM. Field-emission properties of novel palladium nanogaps for surface conduction electron-emitters. *Nanotechnology* 2007;18:475708.
- [8] Lo HY, Li Y, Tsai CH, Chao HY, Pan FM. Effect of process variation on field emission characteristics in surface conduction electron-emitters. *IEEE Trans Nanotechnol* 2008;7:434–9.
- [9] Lewis FA. The palladium/hydrogen system. London: Academic Press; 1967.
- [10] Zhong W, Cai Y, Tomanek D. Mechanical stability of Pd–H systems: a molecular dynamics study. *Phys Rev B* 1992;46:8099–109.
- [11] Aoyagi M. Temperature characteristics of stress-induced migration based on atom migration. *J Vac Sci Technol B* 2005;23:2384–9.
- [12] Zhai CJ, Blish RC. A physically based lifetime model for stress-induced voiding in interconnects. *J Appl Phys* 2005;97:113503–8.
- [13] Goth Y, Ohtake T, Fujita N, Inoue K, Tsuji H, Ishikawa J. Fabrication of lateral-type thin-film edge field emitters by focus ion beam technique. *J Vac Sci Technol B* 1995;13:465–8.
- [14] Tsai CH, Pan FM, Chen KJ, Wei CY, Liu M, Mo CN. Nanogap formation by palladium hydrogenation for surface conduction electron emitters fabrication. *Appl Phys Lett* 2007;90:163115–7.
- [15] Tsai CH, Chen KJ, Pan FM, Lo HY, Li Y, Liu M, et al. Nanogap fabrication on palladium electrodes for FED applications. *SID Symp Digest* 2007;38: 583.
- [16] Li Y, Lo HY. Surface conduction electron emission in palladium hydrogenation nanogaps. *J Phys D: Appl Phys* 2008;41:085301.
- [17] Lo HY, Li Y, Chao HY, Tsai CH, Pan FM, Kuo TC, et al. Three-dimensional simulation of novel surface-conduction electron emitter. *SID Symp Digest* 2007;38:586.
- [18] Li Y, Chao HY, Lo HY. High field emission efficiency surface conduction electron emitters. *J Comput Electron* 2008;7:440–4.
- [19] Li Y, Cheng H-W. Field emission stability of anodic aluminum oxide carbon nanotube field emitter in the triode structure. *J Nanosci Nanotechnol* 2009;9:3301–7.